CLM - P 382

This document is intended for publication in a journal, and is made available on the understanding that extracts or references will not be published prior to publication of the original, without the consent of the authors.

CLM - P 382

CULHAM LABORATORY
LIBRARY
6 MAY
D
IDAIC

UKAEA RESEARCH GROUP

Preprint

SERVO CONTROL OF PLASMA POSITION IN CLEO-TOKAMAK

J HUGILL
A GIBSON

CULHAM LABORATORY
Abingdon Berkshire

1974

Enquiries about copyright and reproduction should be addressed to the
Librarian, UKAEA, Culham Laboratory, Abingdon, Berkshire, England

CLM-P 382

SERVO CONTROL OF PLASMA POSITION IN CLEO-TOKAMAK

J. HUGILL

A. GIBSON

(Submitted for publication in Nuclear Fusion)

A B S T R A C T

A system for servo-control of the plasma position in a tokamak discharge is described. Measurements of the stability boundary of the servo-loop in the Cleo-Tokamak apparatus are presented, and compared with a theoretical model. They show reasonable agreement. Using servo-control, the discharge time was extended from 110ms to nearly 200ms, and the plasma remained within ± 10mm of the centre of the vacuum vessel for up to 140ms. The instability caused by a deliberately applied vertical field with positive gradient was stabilised.

UKAEA Research Group,

Culham Laboratory,

Abingdon,

Berks

January 1974

1. INTRODUCTION

This paper describes the performance of a system for controlling the position of the current channel in the Cleo-Tokamak apparatus. A general description of the apparatus together with preliminary results have been presented at various conferences [1 - 3]: more details, especially of the control windings and detector circuits, are given in Section 2.

A theoretical analysis of the servo-loop is given in Section 3, and various experimental results compared with the theory in Section 4. Sections 5 and 6 contain a short discussion of the results and conclusions.

Previous work on the control of plasma position by means of windings outside the vacuum vessel, instead of the usual copper shell, [4] has used negative impedance circuits to modify the response of the winding to plasma motion. In other words the control winding is also used to detect the plasma motion. Using this technique it is not possible to reduce the effective circuit resistance to zero, otherwise the circuit becomes unstable, so the plasma position can not be held indefinitely. Here we employ separate detection and control windings, whose mutual inductance can be made very small. We could, in principle, use any convenient monitor of plasma position, for example, a multi-channel μ-wave interferometer. The control winding is used in a servo-loop to move the plasma column so as to minimise the difference between the measured position and that required, and the required position may be held indefinitely.

The same system can be used to simulate the effect of a perfectly conducting shell, by controlling the flux through a surface external to the plasma, measured by a suitable sensing coil.

2. DESCRIPTION OF THE APPARATUS

Briefly, the apparatus is a tokamak without a copper shell in which equilibrium is provided by an externally applied time-varying vertical field. The time for vertical field penetration of the stainless steel vacuum vessel is approximately 1ms.

The vertical field arises from several windings which are shown in Fig. 1. A magnetometer survey was made of the field produced by each winding in the presence of the steel transformer core: its magnitude and variation with major radius. With the core biassed up to 80% of saturation, the field was a linear function of current and the field produced by two or more windings could be added linearly.

Hysterisis effects were negligible. The attraction of the plasma to the core was also estimated by comparing the magnetic field of a copper ring, simulating the plasma current, with and without the transformer core present. These results are presented in Table I.

The arrangement of the primary circuit is shown in Fig. 2. The 'vertical field winding' D, compensated by an equal and opposite number of turns on the core, is placed in series with the primary winding, and shunted by an inductive shunt. Adjustment of the shunt resistance provides control of the steady value of the vertical field, and the shunt inductance, in addition to compensating the inductance of the vertical field winding and the mutual inductance between the plasma circuit or primary and the vertical field winding, also provides some degree of control of the time behaviour of the ratio of vertical field to plasma current.

The position of the discharge current channel is monitored by a combination of the signals from two separate coils wound on the outside of the vacuum vessel. These are depicted schematically in Fig. 3. One is a simple saddle-coil or loop arranged to pick up the total vertical flux through the vacuum vessel, and the other is similar to a conventional Rogowski coil but with the number of turns per unit length varying as the cosine of the minor azimuthal angle. These coils are both sensitive to displacement of the current channel and to vertical field. After integration their response is of the form,

$$V_c = AI\,(R - R_1) + CB_z$$

$$V_s = DI\,(R - R_2) + EB_z \qquad (1)$$

where A, C, D, E, R_1, R_2 are constants, I is the discharge current, R is the major radius of the discharge, and B_z is the externally

applied vertical field. By combining the signals from the two coils either before or after integration we can effectively solve equations (1) and obtain

$$I(R - R_x) = (EV_c - CV_s)/\Delta \qquad (2)$$

$$B_z/I = K-(DV_c - AV_s)/\Delta I \qquad (3)$$

where $\Delta = AE - CD$

$$R_x = (AER_1 - CDR_2)/\Delta \qquad (4)$$

and $K = AD\ (R_2 - R_1)/\Delta$

Because of toroidal effects R_x does not equal the major radius of the torus, R_o, but we may write (2) as

$$I\ (x - x_o) = (EV_c - CV_s)/\Delta \qquad (5)$$

where x is the displacement of the current channel from the center of the vacuum vessel, and x_o is a constant. We call the l.h.s. of equation (5) the position coil signal. Notice that it does not depend on B_z, so that the possibility of accidental feedback due to coupling between the control winding and the position monitor can be eliminated.

The cosine and saddle coils were calibrated on the bench using a thin circular coil of the same major diameter to simulate the plasma current, and a Helmholz pair to provide vertical field. Instead of changing the major radius of the current simulator it was displaced with respect to the center of the coils being calibrated. For small displacements this does not cause appreciable error. By this method the constants in equation (1) are evaluated, from which the sensitivity of the combination can be derived.

An exactly similar set of coils rotated through 90^o is used to

monitor the vertical position of the current channel; and three pairs of these position monitors are placed around the major circumference of the vacuum vessel at positions 1, 2, 3 in Fig. 1.

Experimentally we find that the plasma position recorded by each set of coils is the same within an experimental error of about $\pm$ 3mm, even when the plasma is displaced by more than 60mm from the center of the vacuum vessel. In other words during vertical and radial plasma motion the center of the current channel appears to coincide closely with a field line of the toroidal field. For macroscopic motion it appears that the plasma has only two degrees of freedom. This, of course, makes the control of its position very much simpler. Strictly speaking, we can not make such a statement during the disruptive instability, which occurs in our machine for values of the safety factor at the limiter $q_L < 4$. The time scale of this instability is $\sim$ 100 μs, whereas the detection time of the position monitors is about 1ms, the time for vertical field to penetrate the vacuum vessel.

The control windings, shown at F in Fig. 1, consist of 4 separate windings which can be connected to provide either vertical or radial field in the region of the plasma. Three of these windings are used for vertical field. Each is driven by a pair of transistor power amplifiers in push-pull and the whole winding can supply up to $\pm$ 20 Gauss, or $\pm$ 10% of the total vertical field required for equilibrium at 70 kA plasma current. The input to the power amplifiers is an amplified 'error' signal derived from one of the position monitors (position 3 Fig. 1), with a small correction added for the offset, x_o, from the normal Rogowski coil for plasma current. A schematic of the complete servo-loop is shown in Fig. 4. The main effect

of the servo-loop in normal operation is to reduce the displacement of the plasma and extend the duration of the current pulse.

We have also successfully used a signal from the saddle-coil alone for this purpose. In this case the servo-loop is connected so as to maintain zero flux through the saddle-coil, that is, to make this coil approximately coincide with a magnetic surface. The general behaviour is similar, but the position coil shows an outward displacement from the center of the vacuum vessel of 16 ± 5mm [1] at peak current, increasing as the current decays. Not many results were obtained with this configuration, and it will not be discussed further.

A very similar servo-loop is used to control the vertical motion of the plasma. Only one control winding is used, connected to give a radial field up to $\pm$ 6 Gauss. This is found most useful in off-setting the effect of stray radial fields from the core, caused by slight non-symmetries in the winding arrangements, but is not powerful enough to cope with the results of core saturation.

3. ANALYSIS OF THE SERVO-LOOP

First we consider the equilibrium and stability of the plasma in the externally applied field alone. This problem has been fully treated by Shafranov [5] and Greene et al [6], and we shall use their results to obtain an equation for the radial motion of the plasma.

---

[1] This agrees well with the value of 14 ± 2mm given by equation (1) with V(saddle) = 0 and $B_z/I = 3.0 \pm 0.1$ Gauss/kA: the value required for equilibrium in this configuration, calculated from Table I. The displacement of the plasma boundary and the magnetic axis given by Shafranov's formulae, [5] with $\beta_\theta = 0.4$, $\ell_i = \frac{1}{2}$ are 6.4mm and 16.8mm respectively.

The equilibrium can be considered as a balance between the expansive force due to the free magnetic energy of the current, I and the plasma pressure, and the inward force due to the interaction of the current with the externally applied vertical field, B_z. The attraction of the plasma to the steel transformer core is equivalent to an external field produced by magnetisation of the core (line 6, Table I), and is included in B_z. The net outward force on the plasma is then,

$$f = 2\pi RI\ (B_{ze} - B_z) \qquad (6)$$

where B_{ze} is the vertical field required for equilibrium, and is given by the models of Shafranov and Greene et al.

$$B_{ze} = \frac{\mu_o I}{4\pi R}\ \Gamma \qquad (7)$$

where $\Gamma = \ell n\ (8R/a) - 3/2 + \ell_i/2 + \beta_\theta$ and $\mu_o \ell_i/4\pi$ is the internal inductance of the current channel per unit length.

For small displacements from equilibrium, $\Delta R = (R - R_o)$, the equation of motion is

$$\frac{d^2R}{dt^2} = \frac{1}{M}\ \frac{df}{dR}\ (R - R_o) = -\ \Omega_F^2\ (R - R_o) \qquad (8)$$

M being the total plasma mass.

In our apparatus the currents producing the external vertical field (gradient $\frac{R}{B}\ \frac{dB}{dR} = m$) are tightly coupled to the plasma current by the ohmic heating transformer, so we take

$$B_z = B_{zo}\left(\frac{I}{I_o}\right)\left(\frac{R}{R_o}\right)^m \qquad (9)$$

Subscript o refers to the equilibrium.

We shall also assume that the plasma conserves toroidal flux, so that

$$\left(\frac{a}{a_o}\right)^2 = \frac{R}{R_o} \qquad (10)$$

and that the plasma current varies as R^n.

$$\frac{I}{I_o} = \left(\frac{R}{R_o}\right)^n \qquad (11)$$

If the plasma conserves poloidal flux we should have $n = -1$, but, because of the large inductance in series with the plasma in our configuration, I could vary less rapidly with R so that

$$0 > n > -1 \qquad (12)$$

In spite of the current redistribution this would imply we still assume ℓ_i is constant and β_θ is constant. There is some support for the latter constraint in the experimental results of the A.T.C. device [7]. A properly self consistent model should take into account all the constraints on the plasma, including the effect of the limiter or vacuum vessel walls in defining the plasma boundary.

Using (7), (9), (10) and (11) to express (6) in terms of R and differentiating, we find

$$\Omega_F^2 = \frac{\mu_o I_o^2}{2R_o M} \left[(1 + m)\Gamma_o - \tfrac{1}{2}\right] \qquad (13)$$

Evidently for $\Omega_F^2 > 0$ stable oscillations of frequency Ω_F can occur, while for $\Omega_F^2 < 0$ the equilibrium is unstable. The condition on m for stability is

$$m > -1 + \frac{1}{2\Gamma_o} \qquad (14)$$

This may be compared with the results of Greene et al [6], equations (124) and (126) for different sets of constraints. It will turn out that the precise value of Ω_F^2 does not have a big effect on the control loop, provided it is positive.

Motion in the vertical direction is simpler to treat if we neglect constraints which may be imposed by boundary conditions at the limiter or vacuum vessel wall. For a vertical field varying as R^m the radial component at distance z above the median plane is

given to first order, by

$$B_R = \frac{mzB_z}{R_o} \qquad (15)$$

The equation of motion in the vertical direction is then

$$Md^2z/dt^2 = 2\pi R_o B_R I \qquad (16)$$

Using (15) for B_R, (7) for B_z gives a similar equation to (8) with

$$\Omega_F^2 = -\frac{\mu_o I_o^2}{2R_o M} m\Gamma_o \qquad (17)$$

The corresponding condition for stability of vertical motion is

$$m < 0 \qquad (18)$$

In what follows we will not discriminate between horizontal and vertical motion. The analysis will apply equally well to each, with the corresponding value of Ω_F^2 inserted from equation (13) or (17).

In addition to that from the external field, forces on the plasma column due to two other circuits are considered. These are a cosinusoidal current distribution in the vacuum vessel, which is assumed to have a circular cross section coaxial with the plasma, and the control winding. For the purpose of calculating fields and inductances the system is supposed to have a linear axis. Toroidal effects are ignored. Subscripts 1, 2, 3 are used to denote the plasma circuit, the shell (vacuum vessel) and the control winding.

The equation of motion becomes

$$\frac{M}{2\pi R_o}\left(\frac{d^2x}{dt^2} + \Omega_F^2 x\right) = (g_2 I_2 + g_3 I_3) I_1 \qquad (19)$$

where $g_2 I_2$, $g_3 I_3$ are the fields produced by the shell and control winding at the plasma by currents I_2, I_3 respectively, and x is the plasma displacement.

The circuit equations are [2]

$$0 = I_2 R_2 + dL_{21}/dt I_1 + L_{22} dI_2/dt + L_{23} dI_3/dt \qquad (20)$$

$$V = I_3 R_3 + dL_{31}/dt I_1 + L_{23} dI_2/dt + L_{33} dI_3/dt \qquad (21)$$

V is the voltage applied to the control winding terminals, or more properly the open circuit voltage of the amplifier driving the feedback winding. R_3, L_{33} include the output resistance and inductance of the driving amplifier. I_2 is the total current flowing one way in half the shell. The other symbols are self-explanatory.

We write

$$\frac{dL_{21}}{dt} = \frac{dL_{21}}{dx}\frac{dx}{dt} \qquad (22)$$

$$\frac{dL_{31}}{dt} = \frac{dL_{31}}{dx}\frac{dx}{dt}$$

The various inductances are given by

$$L_{22} = \frac{\pi^2}{4}\mu_o R_o = \pi^2 R_o\, bg_2$$

$$L_{23} = \pi^2 R_o\, bg_3$$

$$\frac{dL_{21}}{dx} = 2\pi R_o g_2 \qquad (23)$$

$$\frac{dL_{31}}{dx} = 2\pi R_o g_3$$

and

$$g_2 = \mu_o/4b \qquad (24)$$

where b is the shell radius.

---

[2] For $I \sim R^n$ the ratio $(L_{21} dI_1/dt)/(dL_{21}/dtI_1) \sim n\Delta/R$, where $\Delta \ll b$, is the displacement of the current channel from the position where $L_{21} = 0$. Similarly the ratio $(L_{31} dI_1/dt)/(dL_{31}/dtI_1)$ is small for n given by (12), so the terms $L_{21} dI_1/dt$, $L_{31} dI_1/dt$ have been omitted.

The voltage V is derived from the position monitor signal via the amplifiers in the servo-loop shown in Fig. 4. We take an equation for V of the form

$$t_c \frac{dV}{dt} + V = - \frac{G\mu_o R_{33}}{2\pi b^2 g_3} \, xI_1 \qquad (25)$$

where G is a non-dimensional constant proportional to the gain of the servo-loop, and t_c is the time constant of the detection and amplifier circuits. The negative sign implies the feedback is negative or stabilising when G is positive. In reality the relation between V and xI_1 will be much more complex since several circuits are involved, but in practice one time constant will dominate the circuit, and this will be equated to t_c.

We define

$$k^2 = L_{23}^2 / L_{22} L_{33}$$

$$t_s = L_{22}/R_2 \qquad (26)$$

$$t_f = L_{33} / R_3$$

and $$\Omega_s^2 = \frac{\mu_o I_1^2 R_o}{Mb^2}$$

where t_s, t_f are the intrinsic time constants of the vacuum vessel and control winding and k is the coefficient of coupling between them. Then, taking $I_2 = I_3 = 0$ when x and its derivatives are zero, we obtain, from equations (19) to (26), a fifth order linear differential equation for x.

$$A \frac{d^5x}{dt^5} + B \frac{d^4x}{dt^4} + C \frac{d^3x}{dt^3} + D \frac{d^2x}{dt^2} + E \frac{dx}{dt} + Fx = 0, \text{ where}$$

$$A = t_c t_f t_s (1 - k^2)$$

$$B = t_c(t_f + t_s) + t_f t_s (1 - k^2)$$

$$C = t_c(1 + t_f t_s(1 - k^2)(\Omega_s^2 + \Omega_F^2)) + t_f + t_s$$

$$D = t_c(t_s(\Omega_s^2 + \Omega_F^2) + t_f(k^2\Omega_s^2 + \Omega_F^2)) + 1 + t_f t_s(1 - k^2)(\Omega_s^2 + \Omega_F^2)$$

$$E = t_c\Omega_F^2 + t_s(\Omega_s^2 + \Omega_F^2) + t_f(k^2\Omega_s^2 + \Omega_F^2)$$

$$F = \Omega_F^2 + G\,\Omega_s^2 \qquad (27)$$

We shall be concerned with solutions of the form $x = x_o \exp \lambda t$, where $\lambda = \gamma + j\omega$, is complex.

In practice equation (27) can be simplified to a third order equation because, for the solutions of interest

$$\lambda \sim t_c^{-1},\ t_f^{-1},\ t_s^{-1} \ll \Omega_s,\ \Omega_F \qquad (28)$$

The first two terms of (27) can be negelected, and we have

$$C\lambda^3 + D\lambda^2 + E\lambda + F = 0 \qquad (29)$$

with $C = t_c t_2^2\,\Omega_s^2$

$$D = (t_c t_1 + t_2^2)\,\Omega_s^2$$

$$E = t_c\Omega_F^2 + t_1\Omega_s^2$$

$$F = \Omega_F^2 + G\,\Omega_s^2 \qquad (30)$$

where we have defined

$$t_s(\Omega_s^2 + \Omega_F^2) + t_f(k^2\Omega_s^2 + \Omega_F^2) = t_1\Omega_s^2$$

$$t_s t_f(1 - k^2)(\Omega_F^2 + \Omega_s^2) = t_2^2\,\Omega_s^2 \qquad (31)$$

Ω_s may be recognised as the frequency of oscillation of the plasma within the vacuum vessel if it were perfectly conducting, with no control winding current and neutrally stable external field; for putting $G = 0$, $\Omega_F^2 = 0$, $t_s \to \infty$, $t_f = t_c = 0$ in (27) we obtain

$$\frac{d^3x}{dt^3} + \Omega_s^2 \frac{dx}{dt} = 0$$

A more interesting case is a calculation of the growth rate of the instability which occurs when $\Omega_F^2 < 0$ and $G = 0$, but the control winding is still in circuit, so that currents flowing in this winding complement those induced in the vacuum vessel. $G = 0$, $t_c = 0$ in (29) with $\lambda = \gamma$ gives

$$t_2^2 \Omega_s^2 \gamma^2 + t_1 \Omega_s^2 \gamma + \Omega_F^2 = 0 \qquad (32)$$

whose solution is:

$$\gamma = \frac{- t_1 + [t_1^2 - 4t_2^2 \, \Omega_F^2/\Omega_s^2 \,]^{\frac{1}{2}}}{2t_2^2} \qquad (33)$$

Turning now to the more general case, we can find the conditions that equation (29) has no unstable solutions by applying the Routh-Hurwitz rule [8]. Ω_s^2, t_s, t_f, t_c and $1 - k^2$ are intrinsically positive, and for $\Omega_F^2 < 0$, we assume $t_2^2 > 0$, which will only be invalid for extreme values of m, when $\Omega_F^2 + \Omega_s^2 < 0$. For example, substituting from equations (14) and (17) for Ω_F^2 and from (26) for Ω_s^2 gives

$$\frac{1}{\Gamma_o} \left(\frac{1}{2} + \frac{2R_o^2}{b^2} \right) - 1 < m < \frac{2R_o^2}{\Gamma_o b^2} \qquad (34)$$

for $R_o/b = 4$, $\Gamma_o = 3$ this gives,

$- 11.5 < m < 10.67$, whereas for most practical applications we will have $|m| \leq 2$. The Routh-Hurwitz stability conditions then require D, E, F and DE-CF to be positive. Substitution from equations (30) give the following limitations on gain,

$$G > - \Omega_F^2/\Omega_s^2 \, , \qquad (35)$$

$$G < \frac{t_1}{t_c} + \frac{\Omega_F^2}{\Omega_s^2} \frac{t_1^2}{t_2^2} \frac{t_c}{t_1} + \frac{t_1^2}{t_2^2} \qquad (36)$$

and on the control time constant, which should be less than a linear

function of t_s, t_f, given by

$$t_c < \frac{t_1 \Omega_s^2}{\Omega_F^2} \qquad (37)$$

Fig. 5 shows the stability boundaries in two cases: $\Omega_F^2 < 0$ and $\Omega_F^2 > 0$ for arbitrarily chosen values of t_1, t_2.

We can find the oscillation frequency on the stability boundary by putting $\lambda = j\omega_c$ in (29). The real and imaginary parts of the resulting expression yield

$$E - \omega_c^2 C = 0 \qquad (38)$$

$$F - \omega_c^2 D = 0$$

from which

$$\omega_c^2 = \left(\frac{\Omega_F^2}{\Omega_s^2} + \frac{t_1}{t_c} \right) / t_2^2 \qquad (39)$$

4. EXPERIMENTAL RESULTS

In the usual configuration a 16 turn primary winding is placed at position E on the core (Fig. 1) and a 10 turn vertical field winding, D is compensated by 10 turns at A. The vertical field winding is heavily shunted. The nett field at the plasma is 3.2 ± 0.2 Gauss/kA-t with $m = -0.2 \pm 0.1$. Of this figure three quarters arises from the combined action of the primary and the attraction of the plasma loop by the core, and the remainder is produced by the vertical field winding itself. The shunt value is chosen so that the control winding is operating at a mean current level near zero.

We estimate Γ_o, defined by (7) to be 2.9 ± 0.2 from the field required for equilibrium, given above, which corresponds with $\ell_{i/2} + \beta_\theta = 0.64 \pm 0.2$. The limits on m for radial and vertical stability, given by (14) and (18) are then

$$-0.83 < m < 0,$$

so that the configuration described above should be stable without servo-control. Indeed, as reported earlier [2, 3] we obtain equilibrium for up to 110 ms. With feedback we can extend the pulse length up to 200 ms and keep the current channel centred within $\pm$ 10mm (as measured by the position coil signal) for up to 140 ms.

Late in the discharge, when the current is greater than about 50 - 60 kA, we observe local saturation of the core under the primary winding. This apparently arises because the vertical field flux which the primary winding provides, returns through the outer limbs of the core. When this occurs the plasma position is much less easily controlled, probably because stray fields arising from the core strongly disturb the equilibrium.

In testing the stability of the servo-loop the bandwidth of the feedback amplifiers was first set at its maximum value and the gain increased in steps in successive discharges. Fig. 6 shows the effect on the position signal. At first the deviations of the position from its steady value are decreased, then, as the gain, G is increased further a more or less steady sinusoidal oscillation of the position signal, and corresponding signals in the remainder of the servo-loop, occurs. We assume that G has exceeded the stability boundary at this point. If so the instability is limited by some non-linear effect, not included in the theory of section 3, at a very low level, hardly enough to disturb the gross behaviour of the plasma. For this reason the critical value of G is difficult to determine accurately. As G increases the amplitude of the oscillation rapidly increases but its frequency does not change appreciably.

An alternative explanation is that the low level oscillation is only enhanced narrow-band noise which precedes the true instability threshold as G increases. In either case we can not increase G much further without saturating the amplifier driving the control winding.

In order to test the effect of varying the detection and driver time constant, t_c, capacitors were placed across the feedback resistor of one of the amplifiers in the servo-loop, as shown in Fig. 4. The main effect was to change the frequency of the instability without affecting the critical value of gain. The form of the position signals obtained is shown in Fig. 7. The output voltage of the driving amplifier was also monitored to check that it was not being driven into saturation.

We now compare the results obtained with the theory of Section 3 in more detail. We first check that the assumptions of Section 3 are valid. The plasma conditions corresponding with the results of Figs. 6 and 7 are:

$I_1 > 45$ kA, electron line density $< 1.4 \times 10^{18}$ m^{-1}, $R_o = 0.9m$, $b = 0.2m$

For these parameters assuming one proton mass for each plasma electron, equation (26) gives

$$\Omega_s \geq 2.1 \times 10^6 \text{ radians } s^{-1}$$

From equations (13), (26) we obtain

$$\frac{\Omega_F^2}{\Omega_s^2} = \frac{b^2}{2R_o^2} \left[(1 + m)\, \Gamma_o - \tfrac{1}{2}\right]$$

$= 0.045$ with an estimated error of $\pm$ 0.006 for our parameters.

The time constant of the vacuum vessel, t_s is estimated from a measurement of its D.C. resistance, without allowing for the gap[3].

$$t_s = 0.88 \pm 0.06 \text{ ms.}$$

Using equations (23) for L_{22} and L_{23} and the measured impedance of the control winding/driving amplifier circuit at 15 Hz and at 300 Hz, we can estimate R_3 and L_{33}, taking account of the resistive nature of the vacuum vessel and its coupling to the control winding. From these results we find $L_{33}/R_3 = t_f = 0.63$ ms, $k^2 = 0.21$.

It is difficult to estimate errors on these values which mainly arise from the neglect of toroidal effects and the non-symmetrical disposition of the control winding, but they are thought to be no more than ~ 25%, i.e. the inverse aspect ratio.

Now we can see that the assumptions made in the analysis, that t_s^{-1}, $t_f^{-1} \ll \Omega_F$, Ω_s, are well justified.

We may use the previous results to calculate t_1, t_2 from equations (31) and get

$$t_1 = 1.08 \pm 0.10 \text{ ms}$$

$$t_2 = 0.68 \pm 0.10 \text{ ms}$$

Table II shows a comparison between the critical frequency calculated from equation (39) and the frequency of the instabilities observed for the different values of t_c employed. The detection time constant was assumed to be t_s when the feedback amplifiers were operating broad-band, and equal to the measured response-time of the amplifiers when these were operated with reduced bandwidth. The agreement is not very good, but can probably be accounted for by the approximations

[3] Only 5 cm wide with thick flanges on each side.

made in the theory.

Fig. 8 shows a comparison of the observed and calculated stability boundary in a t_1/t_c v G plot. The errors on the theoretical curves mainly represent the uncertainty in the values of t_1 and t_2. As can be seen, the experimental stability boundary occurs at a value of gain about one quarter of the theoretical one, and which is independent of t_c. A discussion of the discrepancy is postponed until Section 5.

In the second configuration investigated, the primary of 10 turns was positioned on the center limb (A in Fig. 1) and a 16 turn vertical field winding, D was compensated by 16 turns at E. The vertical field winding is not shunted because it provides just enough field for equilibrium. The vertical field gradient, $m = + 2.6 \pm 0.3$. As expected the plasma column is unstable vertically[4]. Whatever value of quasi D.C. radial field is applied the duration of the current pulse is limited to $\sim$ 30 ms. Although the plasma can be nearly centered during the first 10 ms of the discharge it then moves rapidly up or down and, after a further 10 ms, a series of disruptive instabilities begins which causes the current to decrease rapidly. During this phase the plasma often returns to near its central position.

The effect of applying servo-control to the vertical motion is shown in Fig. 9. As the gain of the servo-loop is increased the discharge pulse length increases, and the rate of vertical displacement decreases. The vertical velocity is not brought to zero because there is always some incompletely compensated time-varying radial

---

[4] A similar configuration with $m = + 1.6$ did not show instability for up to 45 ms [3]. In this case an intrinsically weaker instability appears to have been masked by the effects of a non-symmetrical core bias winding and by lack of equilibrium in the radial direction.

field component, probably arising from the core, which eventually results in the saturation of the amplifier driving the control winding, as shown in the figure. When this occurs the gain of the servo-loop of course falls to zero and the plasma again becomes unstable, as indicated by the subsequent, nearly exponential departure of the vertical position from its previous line. Under these conditions the growth rate of the instability is estimated to be

$$\gamma \text{ observed} = 250 \pm 50 \text{ s}^{-1}$$

For vertical motion in this configuration we use equations (17) and (26) to find

$$\frac{\Omega_F^2}{\Omega_s^2} = -0.19 \pm 0.02$$

Equations (31), (33), with $t_f = 0.225$ ms, now give

$$t_1 = 0.723 \pm 0.020 \text{ ms}$$

$$t_2 = 0.358 \pm 0.070 \text{ ms}$$

γ estimated $= 242 \pm 30 \text{ s}^{-1}$, in good agreement with the observed value.

The value of G required theoretically to stabilise the vertical motion is, from (35)

$$G_{min} > 0.19,$$

and from Fig. 9 we can see that this does indeed appear to be sufficient, no instability occurring until after the driving amplifier has saturated, with G = 0.154.

The other stability boundary, from (36) putting $t_c = t_s$ as before, is:

$$G_{max} < 4.0 \text{ at } \omega_c = 2.2 \times 10^3 \text{ s}^{-1}$$

This means that the margin for stability is theoretically very large: $G_{max}/G_{min} \sim 21$. However, experimentally we can see a noticeable increase in the noise level on the output of the driver amplifier in the last trace of Fig. 9 for G = 0.44, so that the practical limit to the gain employed may be very much less than 4.0. This does not appear to be a serious limitation; the position signal in the latter case is within a few mm of the median plane for up to 100 ms.

One unexplained, but possibly significant phenomenon should be mentioned. A set of coils is placed near the gap so as to record the presence of M.H.D. instabilities commonly observed in tokamaks [9]. The envelope of the observed signal is shown in Fig. 9 (d) immediately under the driving amplifier output. When the amplifier saturates an increase in the signal level is observed, often well before the plasma has had time to move appreciably. The relation between the instability amplitude and the state of the servo-loop is not understood. No signals are observed in the servo-loop in the frequency range of the instability, typically 10 kHz, nor would one expect an oscillating field of this frequency to penetrate the vacuum vessel.

5. DISCUSSION

The general agreement between the experimental results and the theoretical model chosen is felt to be good. The main discrepancy is the observation of some low level oscillation which may be non-linearly limited instability, or else enhanced noise, at about 20% of the predicted gain boundary for instability.

The theoretical model could be improved by taking proper account of toroidal effects in calculating the mutual and self inductances

of the plasma, vacuum vessel and control winding. It could be extended to include a better description of the detector circuits than is provided by equation (25), and to include the mutual coupling between the control winding and primary circuit and/or other parts of the structure of the machine. These changes would result in a higher order equation for x than (27) and may change appreciably the instability frequency and the upper gain boundary for stability predicted, but not the gain required to stabilise an intrinsically unstable field configuration, which depends essentially on the D.C. response of the control loop and the value of Ω_F^2. The latter could be improved by a better description of the plasma and of the constraints on it.

It was observed that motion of the feeder cables to the control winding in the presence of the toroidal field could induce voltages comparable with those at the driver amplifier output. Usually the D.C. component of the control winding current pushes the feeder cables against their withholding brackets in 20 - 30 ms, but in its absence, another complication is introduced into the control loop, which would have to be included in a full theory.

6. CONCLUSIONS

We have demonstrated the possibility of positioning a tokamak plasma within a few mm of the center of a concentric stainless steel vacuum vessel (τ = 0.9 ms) by applying a small (up to 10%) correction to the vertical field in a servo-control loop, provided the safety factor, q is sufficiently high to avoid the disruptive instability.

As the gain of the servo-loop is increased the system becomes unstable, and the instability boundary is within a factor of four of that expected theoretically.

The vertical instability induced by applying a vertical field with positive gradient can be prevented by servo-control, with a radial field of only ± 6 Gauss. In this case the gain required agrees well with that calculated theoretically.

ACKNOWLEDGEMENTS

The authors are grateful for the advice and assistance of many colleagues in the course of this work. Mr K.B. Axon made the coils for measuring plasma position and calibrated them; Mr G.W. Reid constructed the control system and together with the Cleo-Tokamak operating team was responsible for machine operations. Dr. J.B. Taylor assisted in the analysis of the control loop; Dr J.W.M. Paul provided experimental time for the measurements; and Dr R.J. Bickerton's encouragement in preparing this paper is much appreciated. Mr B.C. Sanders made the preliminary vertical field survey.

REFERENCES

[1] GIBSON, A. et al, Paper B16-I Third Int. Symp. on Toroidal Plasma Confinement, Garching (1973).
Also: Bull. Am. Phys. Soc. 17 No 11 Paper 2B15 (1972) 985.

[2] PAUL, J.W.M. et al, Paper 1.1.2 Sixth European Conf. on Controlled Fusion and Plasma Phys., Moscow (1973).

[3] HUGILL, J. et al, Paper 1.7.2 Sixth European Conf. on Controlled Fusion and Plasma Phys., Moscow (1973).

[4] ARTEMENKOV, L.I. et al, Paper 1.7.1 Sixth European Conf. on Controlled Fusion and Plasma Phys., Moscow (1973).

[5] SHAFRANOV, V.D., Reviews of Plasma Physics 2, Consultants Bureau, New York (1966) p 103.

[6] GREENE, J.M., JOHNSON, J.L. and WEIMER, K.E., Phys. Fluids 14 (1971) 671.

[7] BOL, K. et al, Paper B12 Third Int. Symp. on Toroidal Plasma Confinement, Garching (1973).

[8] BELLMAN, R.E., GLICKSBERG, I., GROSS, O.A., Rand Corp. Report R-313 (1958) Chapter 2.

[9] MIRNOV, S.V., SEMENOV, I.B., Sov. Atomic Energy 30 (1971) 22.

TABLE I

THE VERTICAL MAGNETIC FIELD STRENGTH IN THE MEDIAN PLANE AT A MAJOR RADIUS OF 0.90 m DUE TO VARIOUS WINDINGS. Refer to Fig. 1 for winding position. The sign of the vertical field is positive when it has the same direction as the flux induced in the central limb of the core.

Winding	Vertical field (Gauss/kA-t)	Gradient $\frac{R}{B_z}\frac{dB_z}{dR}$	Comment
1. A	- 1.89 ± 10%	- 0.63 ± 0.1	
2. E	1.52 "	- 0.16 "	50% variation in major azimuth
3. D-A	6.14 "	+ 0.62 "	
4. D-E	2.73 "	+ 1.91 "	
5. F	23.8	- 1.32	Calculated
6. Simulated plasma ring	-0.84 "	- 0.98 "	From B_z field with and without core

TABLE II

t_c (ms)	ω_c from equation (39) (radians s^{-1})	Observed instability frequency (radians s^{-1})	Ratio
0.88	1670	1880 ± 50	1.13
2.23	1080	760 ± 25	0.70
4.99	759	470 ± 25	0.62

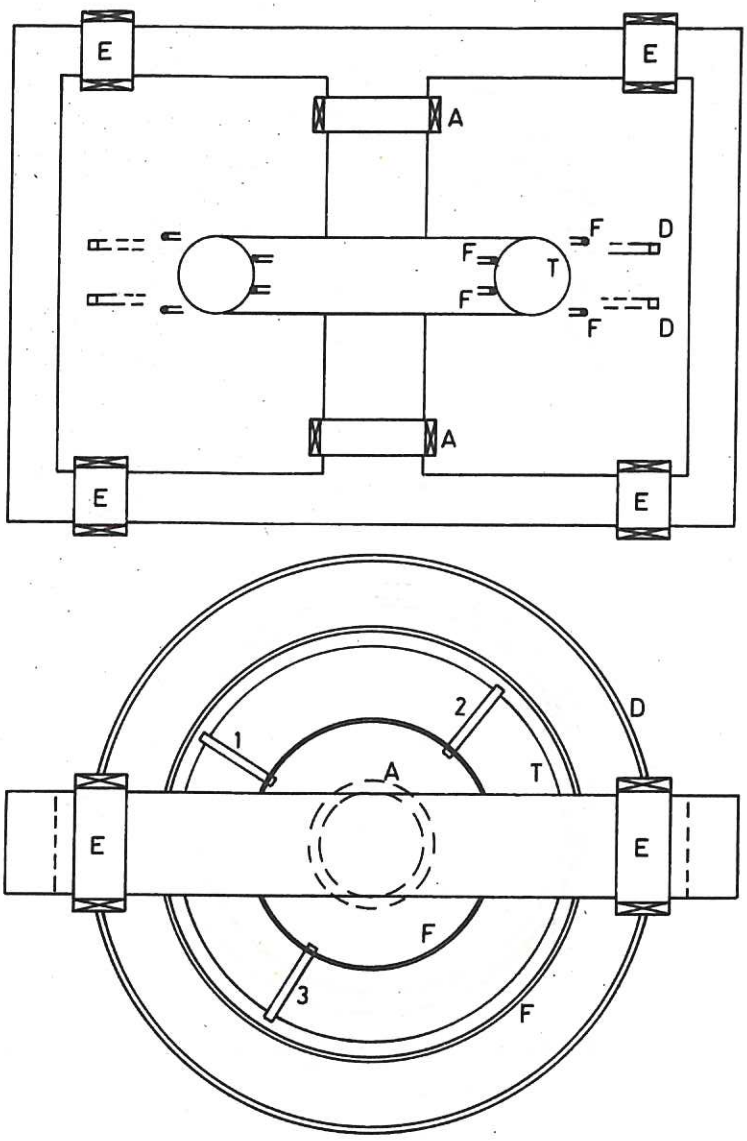

FIG. 1. Showing the positions of various windings on the transformer core, and of the plasma position monitors.

A. 10 turn winding on the central limb.

D. 10 - 16 turn vertical field winding.

E. 16 turn (effective) winding on the horizontal limbs.

F. Control windings producing vertical and radial field.

T. Vacuum vessel.

1, 2, 3 Plasma position monitors.

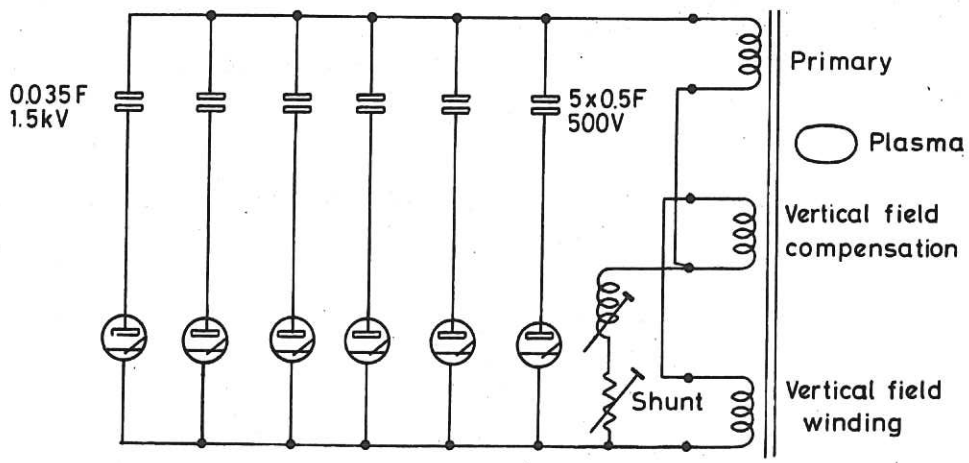

FIG. 2. Simplified schematic of the primary circuit. The capacitors are discharged in sequence into the primary circuit through ignitrons. Capacitor voltages and firing times are varied to control the plasma current waveform.

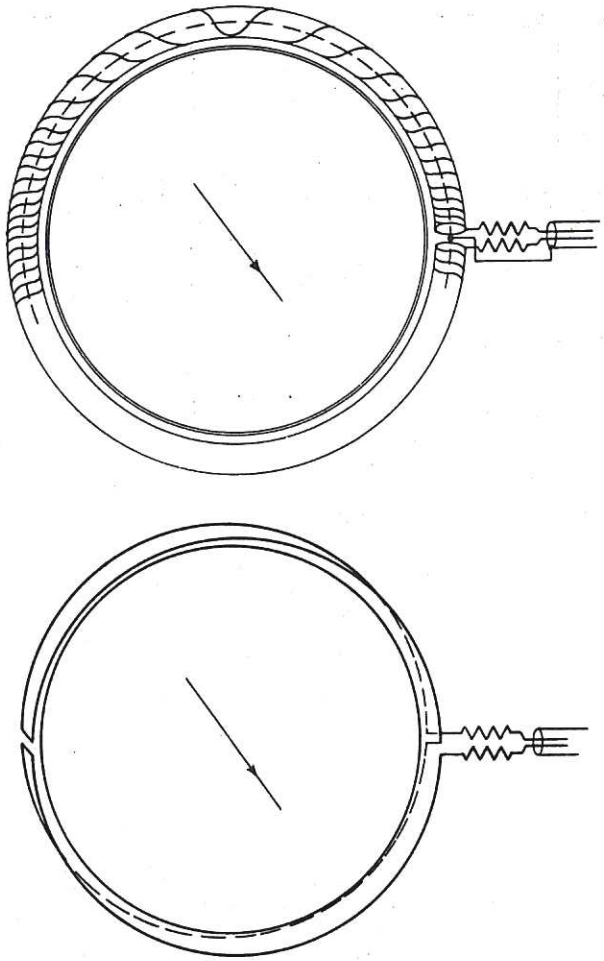

FIG. 3. Sketch of the cosine and saddle coils used for monitoring the radial position of the current channel.

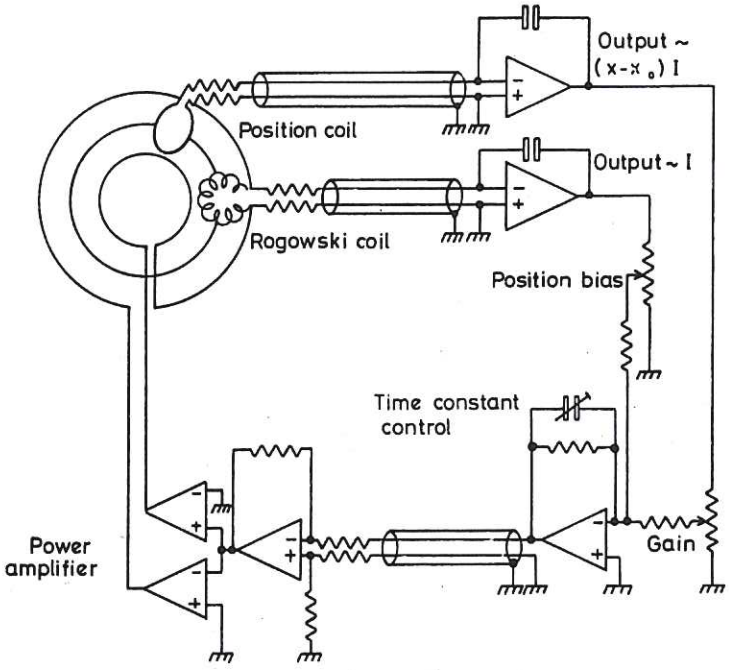

FIG. 4. The servo-loop controlling the radial position of the current channel.

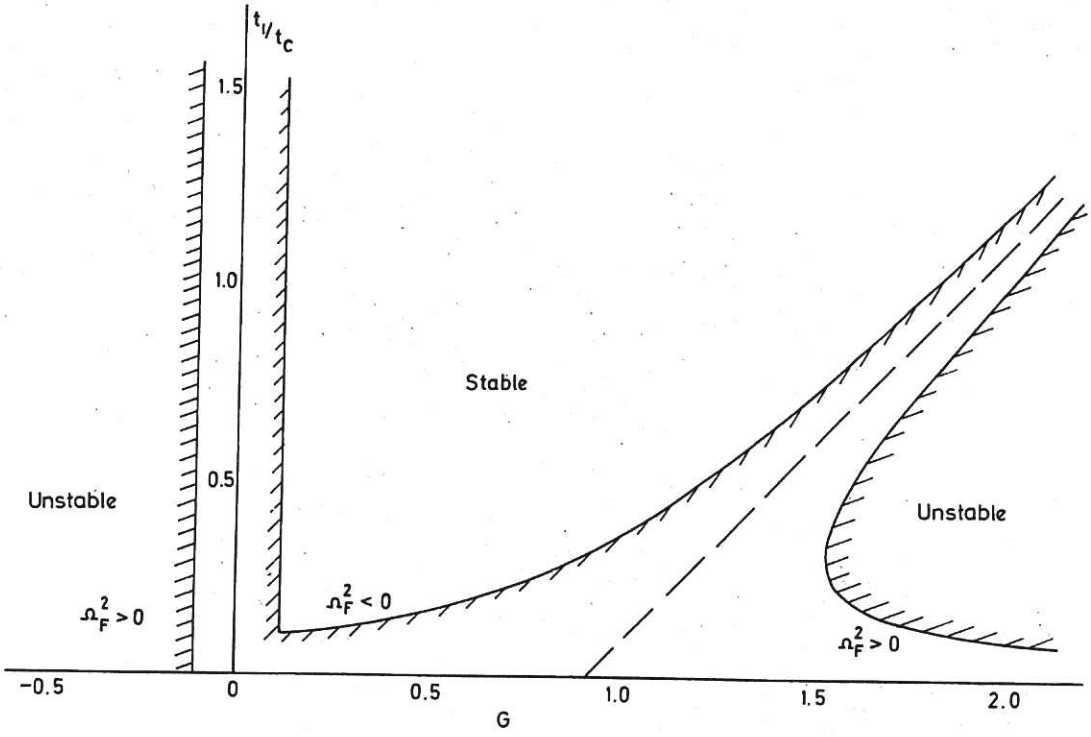

FIG. 5. Stability boundaries in a t_1/t_c v G plot for two cases $\Omega_F^2 > 0$ and $\Omega_F^2 < 0$.

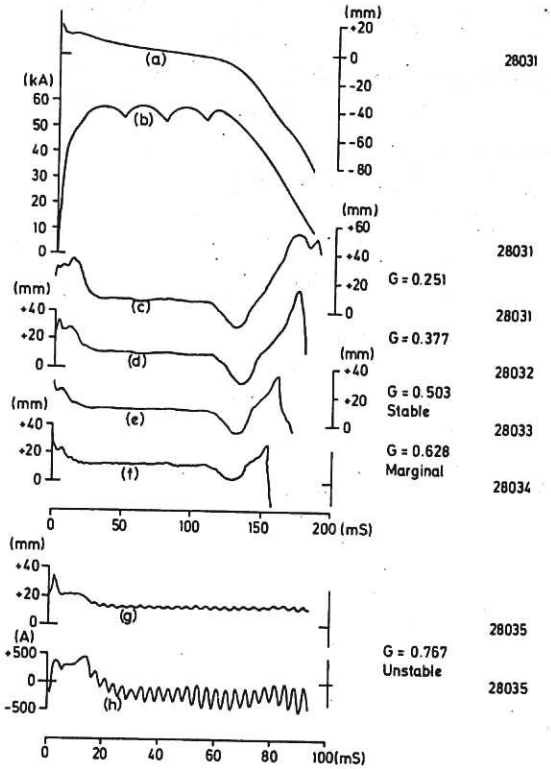

FIG. 6. Experimental result of increasing the gain of the servo-loop on the radial position of the plasma. The traces are, in order from the top: (a) vertical position (positive upwards), (b) plasma current, (c) to (g) radial position (positive outwards) at increasing values of the gain, G and (h) the current in the control winding. The last two traces are on an expanded time scale to show the oscillation better.

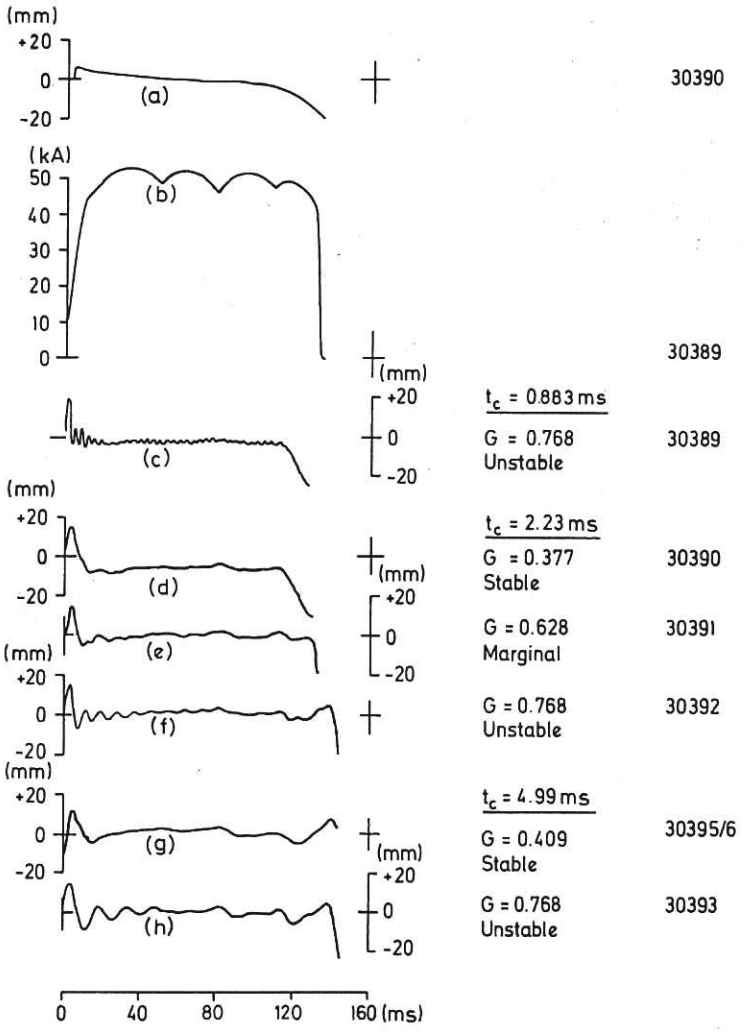

FIG. 7. Behaviour of the radial plasma position at various values of t_c and G. The traces are, in order (a) vertical position (positive upwards), (b) plasma current, (c) to (h) radial position (positive outwards).

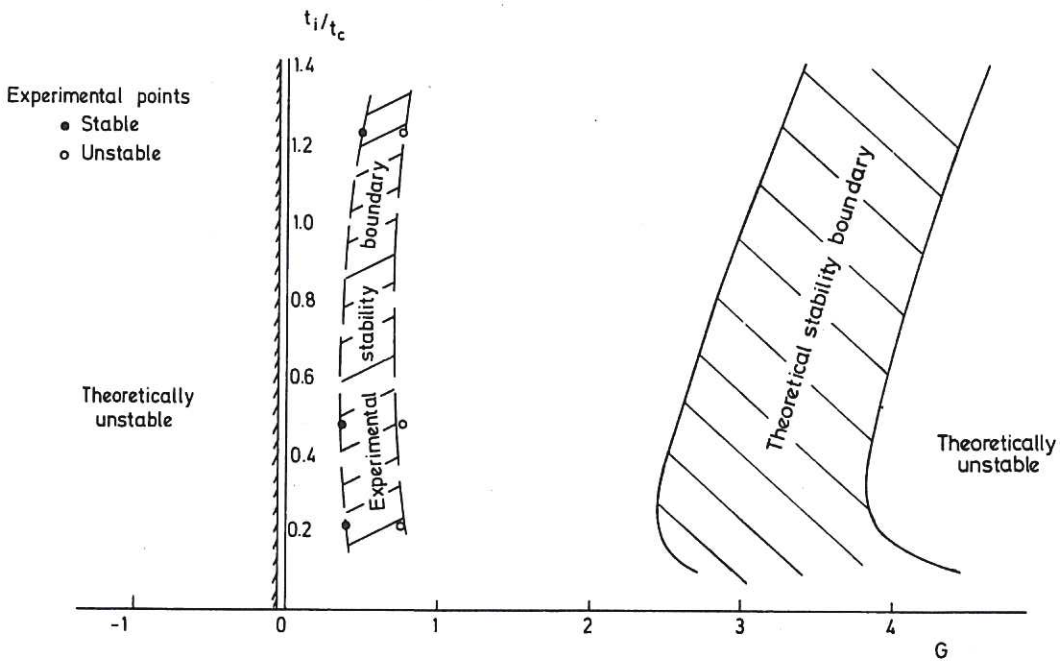

FIG. 8. Comparison of the experimentally determined and theoretically predicted stability boundaries.

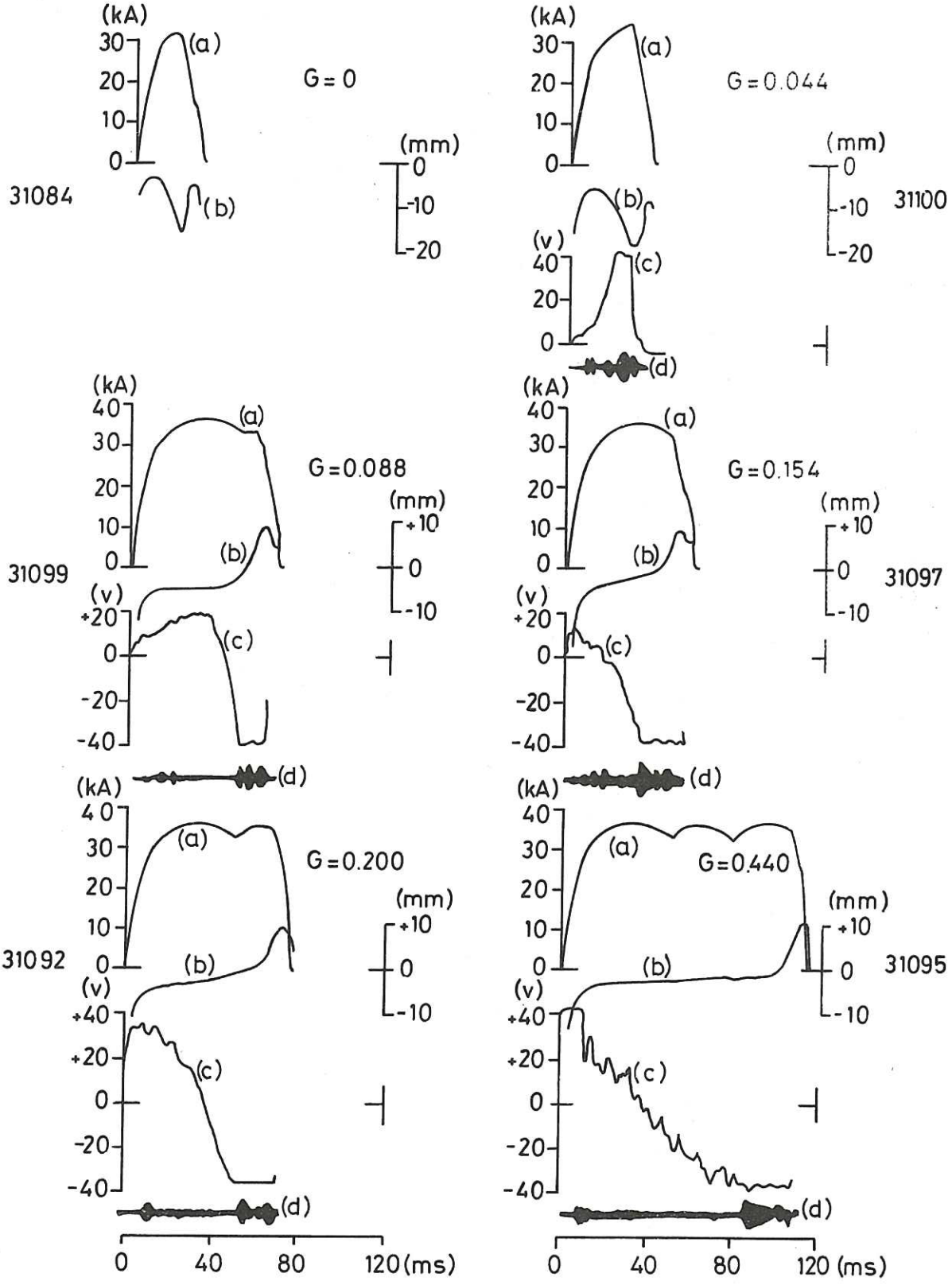

FIG. 9. Illustrating the stabilisation of an unstable vertical field configuration by servo-control of the vertical plasma motion. For each value of the servo-loop gain, G traces of (a) plasma current, (b) vertical position (positive upwards), (c) power amplifier output voltage and (d) the amplitude of M.H.D. oscillations are shown.